# FLEXURAL PERFORMANCE OF EXISTING BRIDGE FOOTINGS SUBJECTED TO SEISMIC LOADS

Y. Yang(1), T. Masuda(2), E. Yoshida(3), S. Horiuchi(4), and T. Kiriyama(5)

*(1) Research Specialist, Public Works Research Institute, y-yang55@pwri.go.jp*
*(2) Collaborating Researcher, Public Works Research Institute, masuda-t574bs@pwri.go.jp*
*(3) Researcher, Public Works Research Institute, e-yoshida@pwri.go.jp*
*(4) Senior Researcher, Public Works Research Institute, horiuchi-s573bt@pwri.go.jp*
*(5) Research Coordinator for Earthquake Engineering, Public Works Research Institute, kiriyama-t673bs@pwri.go.jp*

## *Abstract*

In this paper, to reasonably evaluate the seismic performance of existing bridge footings, the effect of pile arrangement on the bending performance of a footing subjected to lateral seismic loading is mainly investigated by parametric analysis. The results show that the pile location can considerably affect the bending failure pattern of the footing by constraining the yielding extent of footing top bars. For the footing supported by 2 × 2 pile group, when the piles are placed at the center of the sides parallel to the loading direction, the yielding extent of the top bars in the loading direction can be constrained. Similarly, the piles placed at the center of the sides perpendicular to the loading direction can constrain the yielding extent of the top bars in the other direction. The pile placed at the footing center can constrain the extent of yielding of the top bars in two directions.

*Keywords: Existing bridge footing, pile arrangement, bending failure pattern, parametric analysis*

## 1. Introduction

In the 1995 Hyogo-ken Nanbu earthquake of Japan, the highway bridges designed with old standards suffered from destructive damage [1]. To prevent destructive damage and ensure that relief activities run smoothly after an earthquake in the future, a 3-year seismic retrofitting project was conducted from 2005 to 2007 targeting existing highway bridges on emergency transportation roads. The bridge piers were mainly retrofitted in the 3-year seismic retrofitting project. However, when the retrofitted bridge piers have larger capacities than the bridge foundations, it is possible that bridge foundation failure will occur before bridge pier failure during future earthquakes. Thus, seismic performance evaluation and seismic retrofitting of bridge foundations of existing bridges, especially of those with retrofitted piers, is important.

For pile foundations most commonly adopted in existing bridges, footings transfer load from a superstructure to piles, and can largely affect the structural performance of bridge foundations. In old design standards, footings were mainly designed to bear vertical gravity loads. Previous studies also focused on the structural performance of footings subjected to vertical gravity loads. However, with regard to the structural performance of footings under lateral seismic loading, which always leads to cracking and reinforcement yielding at the footing top, the relevant previous studies are very limited. For example, in the reference [2], the theoretical and experimental studies related to the seismic assessment and retrofitting of bridge spreading footings were conducted. To investigate the failure mechanism and bearing capacity of a footing subjected to lateral seismic loading, a four-pile-supported footing specimen, designed based on a prototype bridge footing damaged in the 1995 Hyogo-ken Nanbu earthquake, was tested by Kosa et al. [3]. To further investigate the seismic behavior of footings, 3 four-pile-supported footing specimens with different shear span ratios and reinforcement ratios were tested by Kosa et al. [4].

Furthermore, in most design standards, such as the Design Specifications for Highway Bridges of Japan [5], the footing is approximately considered as beam member in a new bridge design and always designed based on the engineering beam theory-based method, without considering the pile arrangement effect. Although the engineering beam theory-based method is very easily used for footing design, it always leads to conservative evaluation results. The application scope of the beam theory-based method is also unclear. However, for the numerous existing bridges, it is important to accurately evaluate the footing seismic performance to reasonably prioritize their seismic retrofitting, largely different from the footing design of new bridge. When the current beam theory-based method is applied, due to conservative evaluation results, it is difficult to obtain the reasonable seismic retrofitting sequence for the existing bridge footings. As the first step, it is necessary to clarify the failure mechanism of a footing subjected to lateral seismic loading, which has not yet been well understood in previous studies.

In this paper, the effect of pile arrangement on the bending failure pattern of a footing subjected to lateral seismic loading is mainly investigated by parametric analysis. First, a footing static loading test, which was conducted at the Public Works Research Institute of Japan, is introduced. Second, a finite element (FE) analysis is conducted to obtain the basic model for parametric analysis of the pile arrangement effect. Third, based on the basic model, the parametric analysis is carried out to investigate the effect of pile arrangement on the footing bending failure pattern under seismic loading.

## 2. Review of experimental work

### 2.1 Footing specimen

With reference to prototype bridges designed with old standards published before 1980 in Japan, the 1/3 scale four-pile-supported footing specimen shown in Figure 1 was designed. The footing portion has dimensions of 2500 mm×1600 mm×650 mm. The pier portion has cross-sectional dimensions of 600 mm×600 mm and height of 1550 mm. The pile portion has a diameter of 350 mm and length of 300 mm. Piles with shorter lengths are designed to reproduce the reaction force distribution of the pile foundation.

The top reinforcement of the footing portion is 8 bars of D13 parallel to the long side and 14 bars of D13 parallel to the short side; the bottom reinforcement is 16 bars of D19 parallel to the long side and 26 bars of D19 parallel to the short side, respectively. The longitudinal reinforcement of the bridge pier is 24 bars of D32. The transverse reinforcement of the bridge pier is D19 with a spacing of 50 mm. In each pile, the longitudinal and transverse reinforcements are 14 bars of D25 and D13 with a spacing of 50 mm, respectively. The measured material properties of the steel bars and concrete are shown in Table 1.

During the loading test, the four piles of the footing specimen were fixed to a strong reaction floor. To simulate the dead weight of the bridge superstructures, a vertical force of 600 kN was applied by pulling the lower end of a steel rod placed inside the bridge pier. A monotonic loading was applied in the horizontal direction by an actuator at a height of 1 m from the top of the footing.

Further information about the footing specimen can be found in a technical note of the Public Works Research Institute [6].

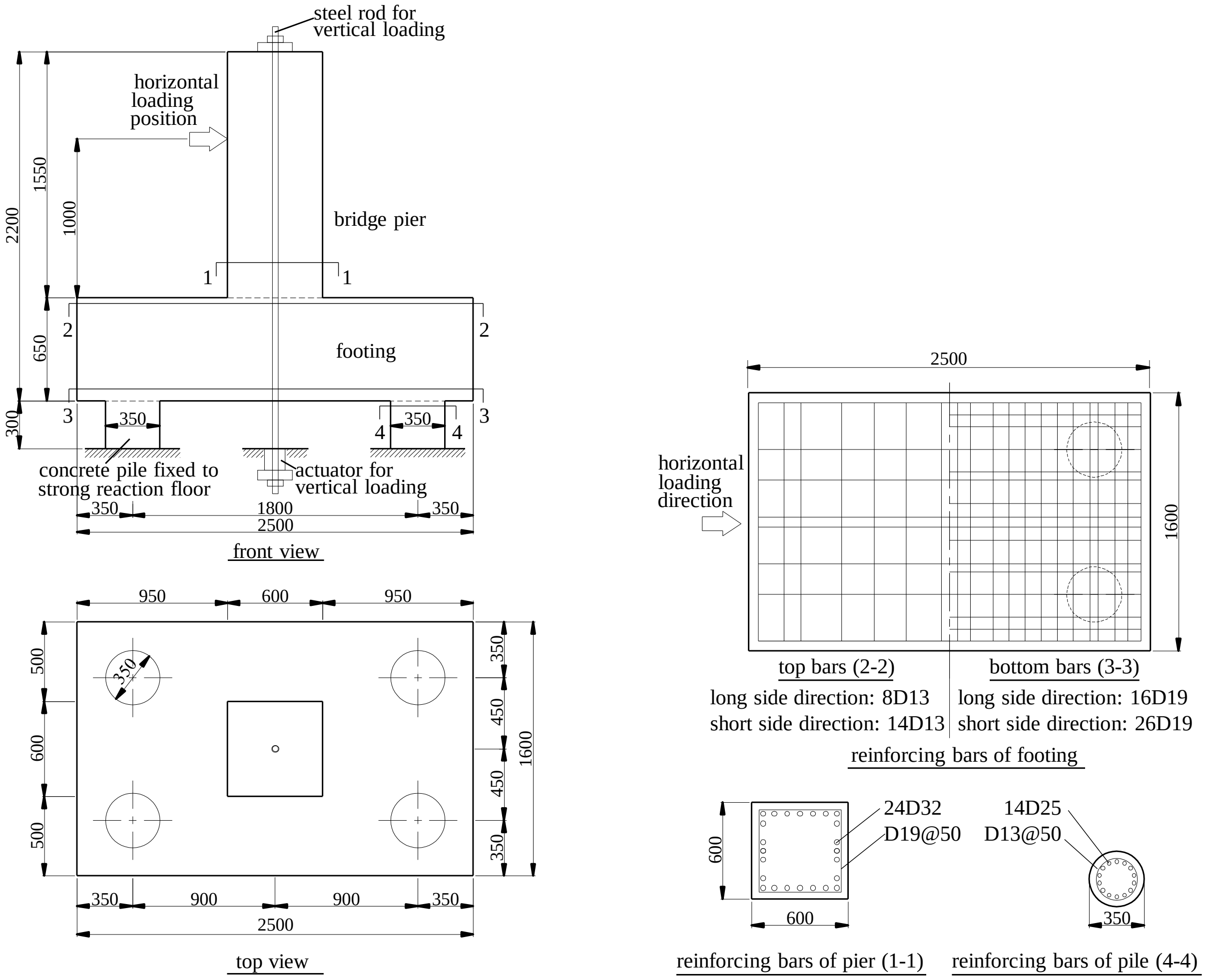


(a) dimension details (b) reinforcing details

Fig. 1 – Details of footing specimen (unit: mm)



 

Table 1 – Material properties

(a) Reinforcing bars

| | nominal diameter (mm) | elastic modulus ($N/mm^2$) | yield strength ($N/mm^2$) | tensile strength ($N/mm^2$) |
|---|---|---|---|---|
| D13 | 12.7 | $1.94\times10^5$ | 397.3 | 584.1 |
| D19 | 19.1 | $1.95\times10^5$ | 364.7 | 584.1 |
| D25 | 25.4 | $1.94\times10^5$ | 405.2 | 595.0 |
| D32 | 31.8 | $1.97\times10^5$ | 372.7 | 557.0 |

(b) Concrete

| | elastic modulus ($N/mm^2$) | compressive strength ($N/mm^2$) | tensile strength ($N/mm^2$) |
|---|---|---|---|
| footing and pile | $2.42\times10^4$ | 32.4 | 2.2 |
| pier | $2.30\times10^4$ | 27.8 | 2.1 |

## 2.2 Main experimental results

The horizontal force-displacement relationship at the loading position is shown in Figure 2. Along with the yielding of the footing top bars ((1) and (2)) placed in the loading direction at the bending verification section, the horizontal rigidity of the footing specimen obviously decreased. After the yielding of the longitudinal bars of the pier ((3)), the loading test was terminated due to insufficient actuator capacity ((4)). Considering that the footing top bars reach a complete yielding status ((2)), reloading was not carried out; thus, there is no deceasing stage shown in the horizontal force-displacement curve. Based on the axial strain of the steel rod measured during the loading stage, which considerably increased near the point of maximum horizontal force ((4)), it is believed that the steel rod served as tension reinforcement to improve the pier capacity during the loading test, resulting in the maximum horizontal force of footing specimen exceeding the selected actuator capacity.

The recorded crack distribution on the surface of the footing portion at the point of maximum horizontal force is shown in Figure 3. The damage near at the bending verification section is considerably greater than that at the other locations.

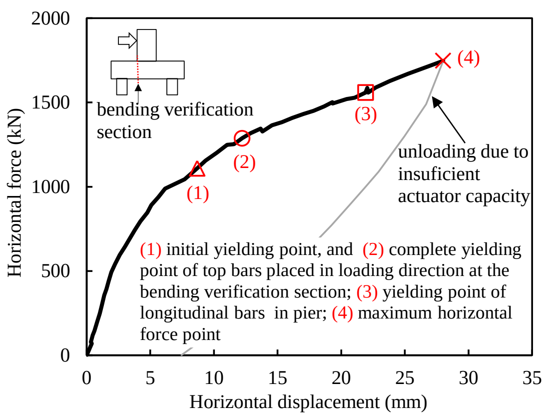


Fig. 2 – Horizontal force-displacement relationship at the loading position

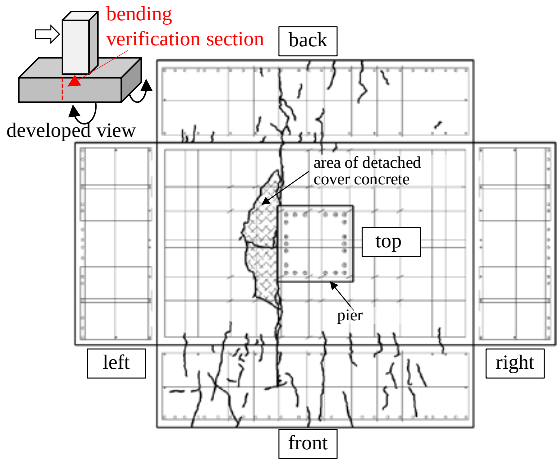


Fig. 3 – Footing crack distribution at the point of maximum horizontal force



 

## 3. Development of the basic model for parametric analysis

### 3.1 Description of the basic model

The basic model for the parametric analysis carried out in Section 4 is developed based on the FE analysis of the loading test, using the program DIANA [7]. The overall geometry of the basic model shown in Figure 4 is identical to that of the experimental specimen (Figure 1). An eight-node isoparametric solid brick element (HX24L in DIANA) is chosen to model the concrete. Based on the preliminary analysis, the mesh size of the concrete element is determined to be 50 mm. The tensile constitutive model of the concrete material proposed in the references [8] and [9] considering tension softening is used. The parabolic curve with a formulation based on fracture energy [10] is adopted for the concrete compressive constitutive model. The reinforcing steels are modeled as embedded bar elements in DIANA and assumed to be elasto-plastic, considering the strain hardening effect. The fixed boundary conditions are applied at the lower end of the piles, as in the loading test.

The vertical force acting on the pier top is simulated by a distributed force, with a resultant force equal to the applied vertical force in the loading test. The horizontal force acting at the same position as that in the loading test is simulated by a displacement-controlled method.

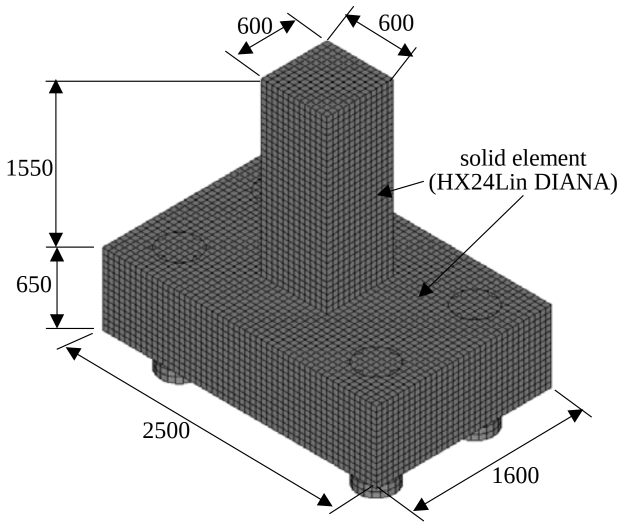


Fig. 4 – FE model (unit: mm)

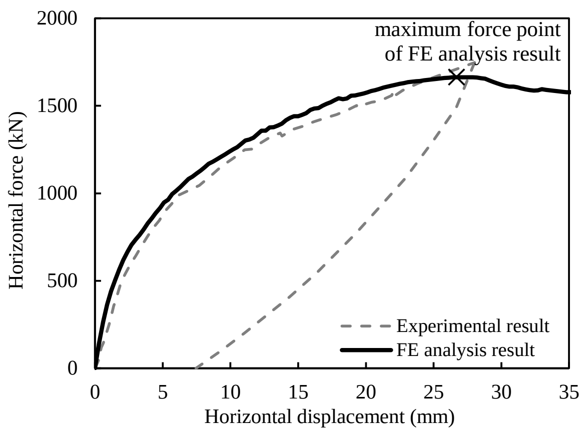


Fig. 5 – Comparison of the horizontal force-displacement relationships between the FE analysis and the experimental results

### 3.2 Verification of the basic model with the experimental results

The comparison of the horizontal force-displacement relationship between the FE analysis and the experimental results is shown in Figure 5. The FE analysis results show good agreement with the experimental results nearly throughout the whole loading stage. Since the steel rod is not modeled and there is no effect on the pier section capacity, the FE analysis result truly reflects the capacity deterioration of the pier section.

At the point of maximum horizontal force, regarding the FE analysis result, the principal tensile strain on the top face of the footing concrete and axial tensile stress of the top bars are shown in Figures 6 and 7, respectively. The principal tensile strain of the footing concrete near the bending verification section is obviously larger than that at other locations, consistent with the crack distribution of the experimental result (Figure 3). The axial tensile stress of the footing top bars also shows a similar distribution trend to that of the



 

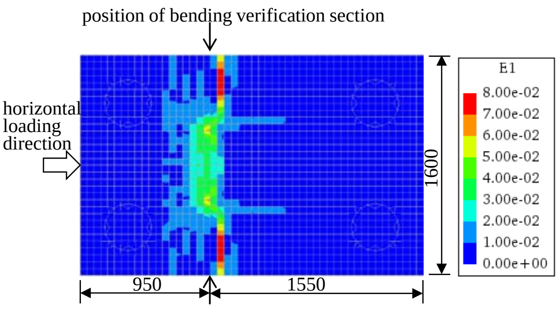


Fig. 6 – Principal tensile strain on the top face of footing concrete at the point of maximum horizontal force

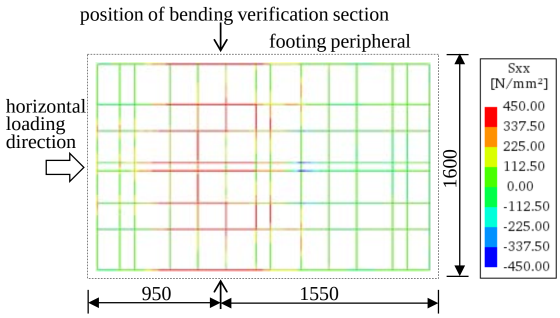


Fig. 7 – Axial tensile stress of footing top bars at the point of maximum horizontal force (yield strength: 397.3 N/mm$^2$)

principal tensile strain of the footing concrete.

Thus, the FE model can accurately predict the overall behavior of a footing specimen and is used as the basic model for the following parametric analysis related to the pile arrangement effect.

## 4. Parametric analysis of the pile arrangement effect

### 4.1 Parameter setting of the pile arrangement

In the current beam theory-based method [5] to evaluate the footing bending capacity, the footing is simply considered as beam member and assumed to have the similar bending failure pattern, without considering the pile arrangement effect. Via a parameter analysis, the effect of piles at different locations on the footing bending failure pattern is investigated.

As shown in Figure 8, two series of footing models are set with different side lengths. In Series 1, with a side-length ratio equal to 1.56, the basic model verified in Section 3 is designated as Case S1-1; Case S1-2 is developed to study the effect of piles placed at the center of the sides parallel to the loading direction on the footing bending damage pattern.

Due to the short length of the side perpendicular to the loading direction in the basic model Case S1-1, no more piles can be placed without creating a spacing less than two and half times the pile diameter, as prescribed in the design standard [5], to consider the pile group effect. Thus, based on the basic model, the models included in Series 2 are developed with longer sides perpendicular to the loading direction, resulting in a smaller side-length ratio equal to 0.96. In Series 2, Cases S2-1 to S2-4 are developed to study the effect of piles placed at the center of not only the sides parallel to the loading direction but also the sides perpendicular to the loading direction. Case S2-5 studies the effect of a pile at the center of the footing on the footing bending damage pattern.

To easily investigate the pile arrangement effect, the footings of the cases included in two series have the same height as that of the basic model. The footing steel ratios at both the top and bottom in two directions are also equal to these of the basic model. In addition, the piles in these cases have the same dimension and reinforcement details. The piers in these cases also have the same details. Furthermore, the vertical forces acting on the piers in these cases are made equal to each other.



 

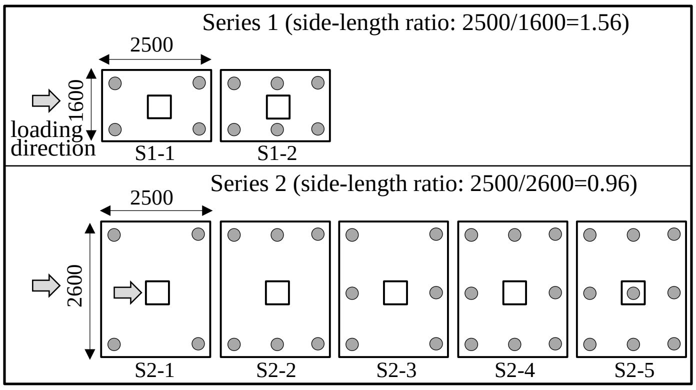


Fig. 8 – Parameter setting of the pile arrangement

## 4.2 Effect of pile arrangement on the horizontal force-displacement relationship of the footing

The FE analysis of the footing models shown in Figure 8 is carried out for the parametric study, under the same analysis settings as that of the basic model described in Section 3.1. The FE analysis results of the horizontal force-displacement relationships at the loading position are shown in Figure 9.

As shown in Figure 9, in Series 1, before the initial yielding of the footing top bars placed in the loading direction, the addition of two piles at the center of sides parallel to the loading direction has little effect on the force-displacement relationship. However, after the initial yielding, Cases S1-2 has larger horizontal rigidity than that of Case S1-1, showing the effect of the additional two piles. Thus, Case S1-2 has a larger horizontal force than that of Case S1-2 after the initial yielding, although the maximum horizontal forces in Cases S1-1 and S1-2 are almost identical, as determined by the longitudinal bars yielding of the pier.

Since a large amount of footing reinforcement is included in the cases of Series 2 to obtain a reinforcement ratio equal to that of Series 1, the piers in Series 2 are modeled with rigid elastic material, to ensure the sufficient development of footing reinforcement yielding. Thus, the maximum horizontal force of each case in Series 2 is determined by the footing instead of the pier. Each case of Series 2 has approximately the same maximum horizontal force, which is controlled by the compressive failure of the

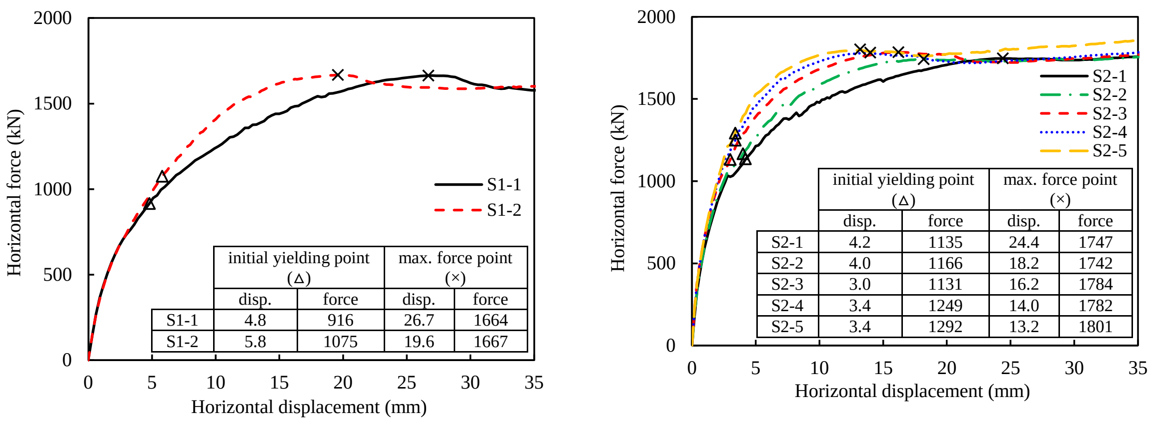


(a) series 1 (b) series 2

Fig. 9 – FE analysis results of the horizontal force-displacement relationships



 

footing. However, before the point of maximum horizontal force, Series 2 exhibits similar results of the force-displacement relationships to Series 1. That is, the pile arrangement can affect the force-displacement relationship after initial yielding. In particular, in Cases S2-2 and S2-3 with the same pile number, the force-displacement relationship of Case S2-2 is obviously different than that of Case S2-3, indicating that pile location is an important parameter affecting the structural performance of a bridge foundation. When the piles are placed at the center of the sides perpendicular to the loading direction, the horizontal rigidity of the bridge foundation can be effectively improved.

### 4.3 Effect of pile arrangement on the bending failure pattern of the footing

Figure 10 shows the yielding extent of footing top bars at the point of maximum horizontal force for each case included in Series 1 and 2, respectively. The results show that the footing bending failure pattern largely depends on the pile arrangement. This finding can be explained by the distribution change of the pile reaction forces (Figure 11). Based on these analysis results, the effect of the piles arrangement on the bending failure pattern of the footing are discussed as follows.

#### 4.3.1 Piles at the center of the footing sides parallel to the horizontal loading direction

In Cases S1-1 and S1-2 of Series 1, as shown in Figure 10(a) and (b), at the point of maximum horizontal force, all the top reinforcing bars placed in the loading direction reach the yielding state at the location near the prescribed bending verification section. However, Case S1-1 exhibits a larger yielding extent than that of Case S1-2, in which the additional two piles are placed at the center of the sides parallel to the horizontal loading direction, although Cases S1-1 and S1-2 sustain approximately the same maximum horizontal force (Figure 9). In other words, the yielding extent of the top bars in the loading direction in Case S1-2 is constrained by the additional two piles. This finding can be explained by the change in the reaction forces of the tensile piles. As shown in Figure 11, due to the effect of the piles placed at the center of the sides parallel to the horizontal loading direction, Case S1-2 exhibits lower vertical reaction forces than those of Case S1-1. At the point of maximum horizontal force, the sum of the vertical reaction forces of the tensile piles 1 and 2 in Case S1-1 is 1324 kN; however, in Case S1-2, the sum of the vertical reaction forces decreases to 770 kN. Thus, the moment acting on the bending verification section in Case S1-2 is smaller than that of Case S1-1. Consequently, in Case S1-2, the footing top bars in the loading direction reach the yielding state later than those in Case S1-1 do, resulting in a smaller yielding extent at the maximum force point.

In Cases S2-1 and S2-2, although the footing top bars placed in two directions yield with a large extent at the maximum force point (Figure 10(c) and (d)), showing a different yielding behavior from that of Series 1, the effect of the piles located at the center of the sides parallel to the loading direction on the footing bending failure pattern can be similarly confirmed. The yielding extent of the top bars placed in the loading direction in Case S2-2 is obviously constrained by the additional two piles, compared with that of Case S2-1. This finding also can be explained by the change in vertical reaction forces in the tensile piles shown in Figure 11(c) and (d).

Furthermore, in Cases S2-3 and S2-4, which have different pile arrangements from that of Cases S2-1 and S2-2, the effect of piles at the center of the sides parallel to the loading direction can also be confirmed (Figure 10(e) and (f)). The change in vertical reaction forces in the tensile piles, which cause the change of the extent of top bar yielding, is shown in Figure 11(e) and (f).

#### 4.3.2 Piles at the center of the footing sides perpendicular to the horizontal loading direction

For Cases S2-1 and S2-3, the yielding extent of the footing top bars at the point of maximum horizontal force is obviously different from each other (Figure 10(c) and (e)). By placing the additional two piles at the center of the sides perpendicular to the horizontal loading direction, the yielding extent of the top bars perpendicular to the horizontal loading direction in Case S2-3 is constrained. This finding also can be explained by the change in the vertical reaction forces of the tensile piles. As shown in Figure 11(c) and (e), although the sums of the vertical reaction forces of the tensile piles are almost identical, the vertical reaction forces of the corner tensile piles, which can affect the yielding extent of the top bars perpendicular to the

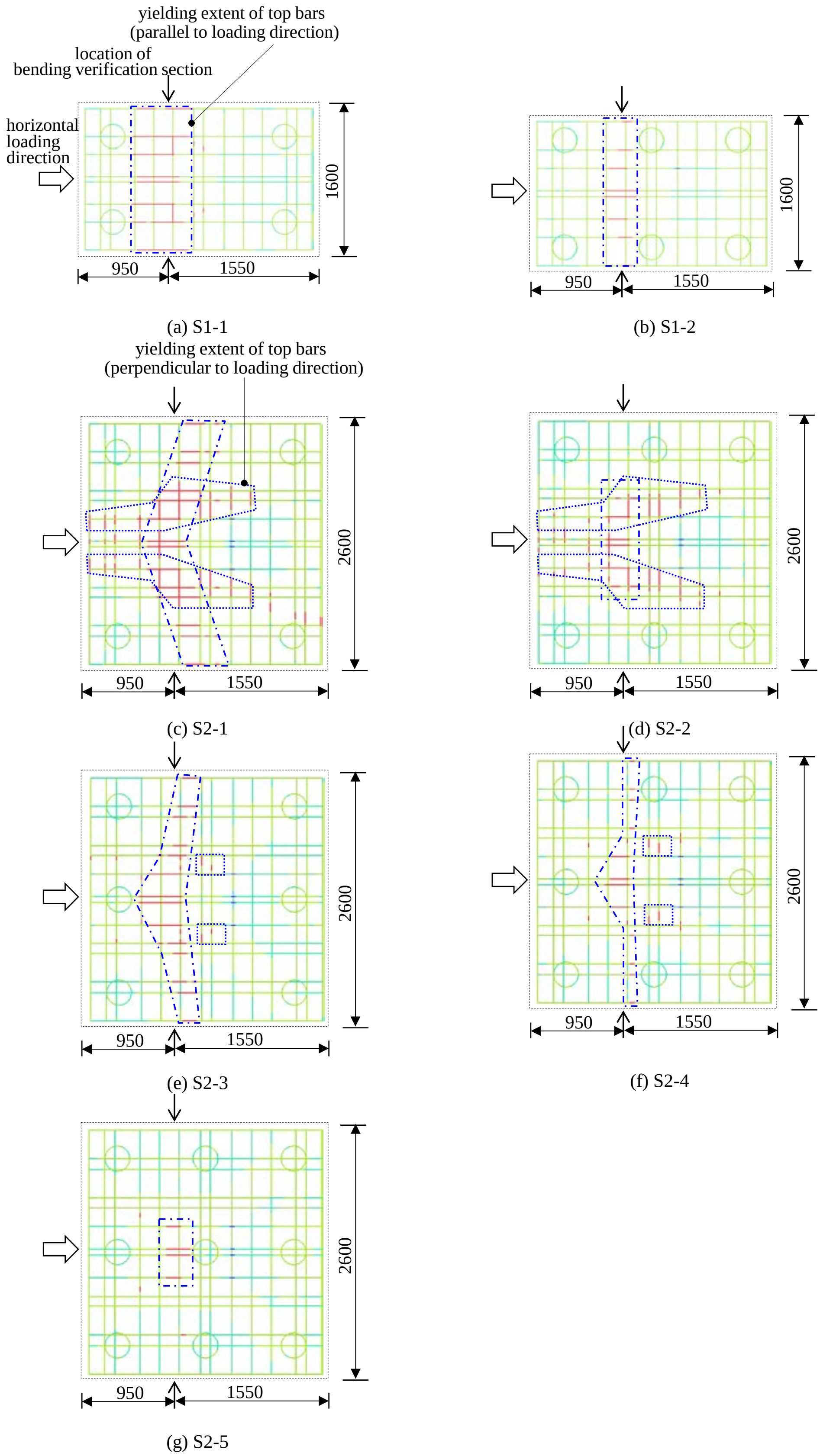


Fig. 10 – Yielding extent of the top bars at the point of maximum horizontal force



 

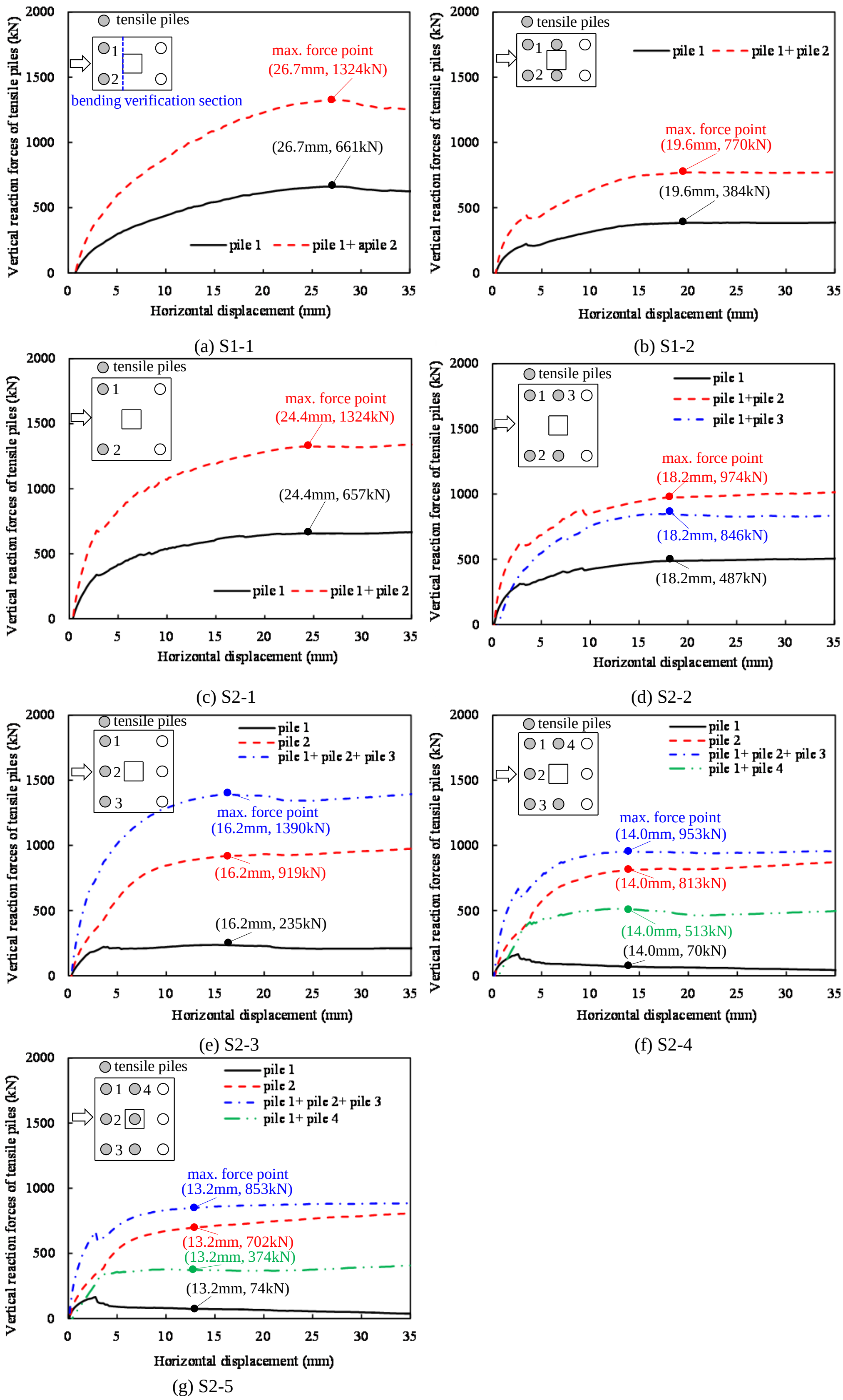


Fig. 11 – Vertical reaction forces of the tensile piles



 

horizontal loading direction, is greatly decreased from 657 kN in Case S2-1 to 235 kN in Case S2-3. Thus, the moment acting on the section parallel to the loading direction is decreased, resulting in the smaller yielding extent of the top bars perpendicular to the horizontal loading direction in Case S2-3.

For Cases S2-2 and S2-4, the effect of the piles at the center of the side perpendicular to the loading direction on the yielding extent of the top bars is similarly confirmed (Figure 10(d) and (f)). This finding also can be explained by the change in the vertical reaction forces of the tensile piles (Figure 11(d) and (f)).

### 4.3.3 Pile at the center of the footing

As shown in Figure 10(f) and (g), compared with Case S2-4, the yielding extent of the footing top bars in two directions in Case S2-5 are constrained by the pile placed at the footing center. This difference can be explained by the change in the vertical reaction forces in the tensile piles. As shown in Figure 11(f) and (g), the sum of the vertical reaction forces of tensile piles 1 to 3, which can affect the yielding extent of the steel bars parallel to the loading direction, is decreased from 953 kN in Case S2-4 to 853 kN in Case S2-5; the sum of the vertical reaction forces in tensile piles 1 and 4, which can affect the extent of yielding of the bars perpendicular to the horizontal loading direction, is decreased from 513 kN in Case S2-4 to 374 kN in Case S2-5. Consequently, the yielding extent of the footing top bars in two directions is constrained in Case S2-5.

### 4.3.4 Summary of the pile arrangement effect on the bending failure pattern of the footing

Based on the above analysis results, the effect of pile arrangement on the footing bending failure pattern can be generally summarized, as shown in Figure 12. For the footing supported by 2 × 2 pile group, when the additional piles are placed at the center of the sides parallel to the loading direction ((1) and (4)), the yielding extent of the top bars placed in the loading direction near the bending verification section is constrained. When the additional piles are placed at the center of the sides perpendicular to the loading direction ((2) and (3)), the yielding extent of the top bars placed in the other direction is constrained. When the additional pile is placed at the center of the footing ((5)), the extents of yielding of the top bars in two directions are constrained.

In other words, the bending failure pattern of the footing can be controlled by the pile arrangement. When the spacing of the tensile piles at the side perpendicular to the loading direction is properly adjusted ((2) and (3)), the main yielding of the footing is controlled to the top bars placed in the loading direction, near at the bending verification section, showing the similar bending failure pattern of beam as assumed in the design stage.

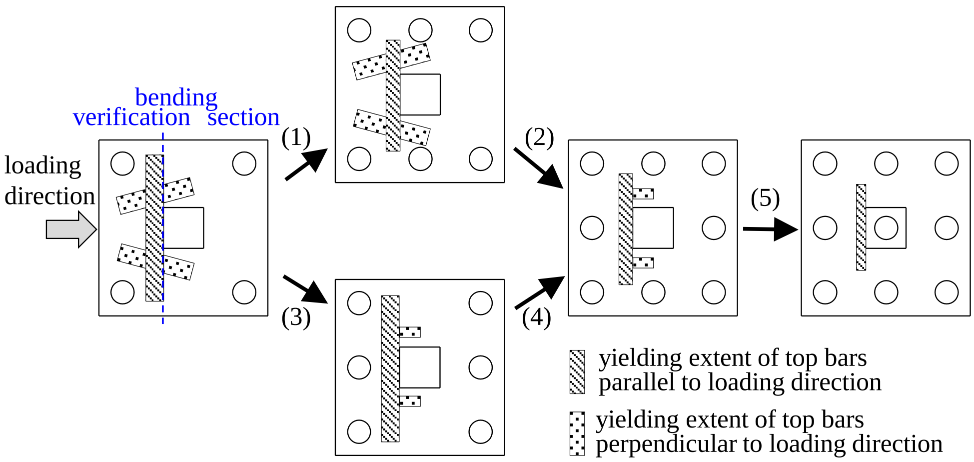


Fig. 12 – Change in yielding extent of footing top bars with pile arrangement



 

## 5. Conclusions

Based on the basic FE model of the footing verified with the experimental results, a parametric analysis was carried out to investigate the effect of pile arrangement on the bending failure pattern of a footing subjected to lateral seismic loading. The major conclusions are obtained as follows.

(1) The FE model was verified with the experimental results to be able to accurately predict the overall behavior of a footing specimen under lateral seismic loading, and can be used as the basic model for the parametric analysis related to pile arrangement effect.

(2) Based on the parameter analysis results, it is confirmed that after the initial yielding point of footing top steel bars, the pile arrangement can largely affect the horizontal rigidity of bridge pile foundation.

(3) The pile arrangement can largely affect the bending failure pattern of a footing. For the footing supported by $2 \times 2$ pile group, the piles additionally placed at the center of the sides parallel to the loading direction can constrain the yielding extent of the top bars placed in the loading direction. Similarly, the piles placed at the center of the sides perpendicular to the loading direction can constrain the yielding extent of the top bars placed in the other direction. The pile placed at the footing center can constrain the yielding extent of the top bars in two directions.

## 6. References

[1] Kawashima K and Unjoh S (1997) The damage of highway bridges in the 1995 hyogo-ken nanbu earthquake and its impact on japanese seismic design. Journal of Earthquake Engineering 1(3): 505–541.

[2] Xiao Y, Priestley MJN and Seible F (1996) Seismic assessment and retrofit of bridge column footings. Structural Journal 93(1): 79–94.

[3] Kosa K, Kobayashi K, Fujii Y, et al. (1999) Experimental study of ultimate behavior of footing due to earthquake load. Journal of Structural Engineering 45A: 1369–1376 (in Japanese).

[4] Kosa K, Fujii Y, Kobayashi K, et al. (2000) Experimental study of footing effected by shear span ratio due to earthquake load. Journal of Structural Engineering 46A: 1405–1412 (in Japanese).

[5] Japan Road Association (2017) Design specifications of highway bridges: part IV Substructure. Tokyo, Japan: JRA (in Japanese).

[6] Public Works Research Institute (2015) Damage Evaluation of Bridge Footings Due to Alkali Silica Reaction and Repair/Reinforcement Approach. Technical Note, No. 4304. Tsukuba, Japan: PWRI (in Japanese).

[7] TNO DIANA BV (2018) DIANA User's Manual (https://dianafea.com/manuals/d102/Diana.html). TNO DIANA BV: Delft, The Netherlands.

[8] Cornelissen H, Hordijk D and Reinhardt H (1986) Experimental determination of crack softening characteristics of normal weight and lightweight. Heron, 31(2): 45-46.

[9] Hordijk D (1991) Local approach to fatigue of concrete. PhD Dissertation. Delft University of Technology : Delft.

[10] Feenstra P (1993) Computational aspects of biaxial stress in plain and reinforced concrete. PhD Dissertation. Delft University of Technology : Delft.



 